Journal of Volcanology and Geothermal Research 189 (2010) 340–346

Contents lists available at ScienceDirect

Journal of Volcanology and Geothermal Research

journal homepage: www.elsevier.com/locate/jvolgeores

A new method to estimate the oxidation state of basaltic series from microprobe analyses

Lydéric France [a,b,*], Benoit Ildefonse [a], Juergen Koepke [b], Florent Bech [c]

[a] Géosciences Montpellier, CNRS, Université Montpellier 2, CC 60, 34095 Montpellier cedex 05, France
[b] Institut fuer Mineralogie, Universitaet Hannover, Callinstrasse 3, 30167 Hannover, Germany
[c] 19 rue des Cuffins, 78830 Bonnelles, France

ARTICLE INFO

Article history:
Received 18 August 2009
Accepted 24 November 2009
Available online 2 December 2009

Keywords:
oxygen fugacity
partition coefficient
clinopyroxene
plagioclase
EPMA
oxybarometer

ABSTRACT

The oxygen fugacity and therefore the iron redox state of a melt is known to have a strong influence on the liquid line of descent of magmas and thus on the composition of the coexisting melts and crystals. We present a new method to estimate this critical parameter from electron probe microanalyses of two of the most common minerals of basaltic series, plagioclase and clinopyroxene. This method is not based on stoichiometric calculations, but on the different partitioning behaviour of Fe^{3+} and Fe^{2+} between both minerals and a melt phase: plagioclase can incorporate more Fe^{3+} than Fe^{2+}, while clinopyroxene can incorporate more Fe^{2+} than Fe^{3+}. For example, the effect of oxidizing a partly molten basaltic system (Fe^{3+} is stabilized with respect to Fe^{2+}) results in an increase of FeO_{total} in plagioclase, but a decrease in the associated clinopyroxene. We propose an equation, based on published partition coefficients, that allows estimating the redox state of a melt from these considerations. An application to a set of experimental and natural data attests the validity of the proposed model. The associated error can be calculated and is on average <1 log unit of the prevailing oxygen fugacity.

In order to reduce the number of different variables influencing the Fe^{2+}/Fe^{3+} mineral/melt equilibrium, our model is restricted to basaltic series with SiO_2<60% that have crystallized at intermediate to low pressure (<0.5 GPa) and under relatively oxidizing conditions (ΔFMQ>0; where FMQ is the fayalite–magnetite–quartz oxygen buffer equilibrium), but it may be parameterized for other conditions. A spreadsheet is provided to assist the use of equations, and to perform the error propagation analysis.

1. Introduction

The oxygen fugacity (fO_2) is a convenient monitor of oxidation state of melts. The oxidation state of a melt is a critical controlling parameter of magmatic processes as it controls the iron redox state of the melt (Kilinc et al., 1983; Kress and Carmichael, 1991; Ottonello et al., 2001; Moretti, 2005; Botcharnikov et al., 2005), and it strongly influences the crystallization sequences and the composition of crystallizing minerals. Grove and Baker (1984) and references therein have shown that the tholeiitic differentiation trend leads to an iron-enrichment of the magma (the "Fenner trend"), while the calc-alkaline differentiation trend, which usually corresponds to more oxidizing conditions, allows the early appearance of oxides thus forcing a silica enrichment (the "Bowen trend"). More recently, Berndt et al. (2005) and Feig et al. (2006) have shown that in a given tholeiitic series, the oxidation state modifies *(i)* the liquidus temperatures of the different mineral phases, and *(ii)* the order of crystallization of mineral phases. In a H_2-buffered system the iron redox state of the melt is closely linked to the H_2O content (e.g., Botcharnikov et al., 2005). Knowledge of the redox state therefore provides information on the evolution of magmatic series (e.g., wet versus dry trends) and on processes/reactions occurring in magma chambers (e.g., Kuritani, 1998; Ginibre et al., 2002; Cordier et al., 2007). The iron redox state of basaltic magmas is also considered to place an upper limit to the fO_2 of their mantle source (e.g., Basaltic Volcanism Study Project, 1981; Carmichael and Ghiorso, 1986; Wood et al., 1990; Carmichael, 1991; Ballhaus, 1993; Ballhaus and Frost, 1994).

Several methods are available to estimate the redox state of a melt (Herd, 2008). In basaltic series, the fO_2 is usually estimated by using the oxybarometer based on the equilibrium between ilmenite and magnetite (Buddington and Lindsley, 1964; Andersen and Lindsley, 1985; Bacon and Hirschmann, 1988; Ghiorso and Sack, 1991; Ghiorso and Evans, 2008; Sauerzapf et al., 2008). However, this method has limitations as coexisting ilmenite and magnetite are not always present in basaltic series. Moreover, oxide minerals are easily reequilibrated at lower temperature (e.g., Venezky and Rutherford, 1999; Koepke et al., 2008; France et al., 2009), either during slow

* Corresponding author. Now at: Géosciences et Environnement Cergy, Université Cergy-Pontoise, 5 mail Gay Lussac, Neuville sur Oise, 95031 Cergy-Pontoise cedex, France.
E-mail addresses: lfrance@um2.fr, lyderic.france@u-cergy.fr (L. France).

0377-0273/$ – see front matter © 2009 Elsevier B.V. All rights reserved.
doi:10.1016/j.jvolgeores.2009.11.023

cooling or during hydrothermal alteration processes. Another method to obtain the fO_2 is the intrinsic fugacity measurement on the bulk rock (e.g., Brett and Sato, 1984). Another common method is to measure the Fe^{3+}/Fe^{2+} ratio (or Fe_2O_3/FeO) of either fresh glasses representing frozen melts, or minerals. For fresh lavas, this ratio can be directly determined from the whole rock composition (e.g., Rhodes and Vollinger, 2005), by measuring both ferrous iron and total iron contents. The alternate solution is to determine the Fe^{3+}/Fe^{2+} ratio in minerals and to calculate the value of the corresponding melt using partition coefficients (Tegner et al., 2003). The Fe^{3+} content in minerals is commonly estimated using formula calculations based on appropriate mineral stoichiometry. However, Canil and O'Neill (1996) and Sobolev et al. (1999) have shown that these calculations for silicates such as clinopyroxene (Cpx) or plagioclase (Pl) are not valid. Therefore, the best way to constrain the prevailing fO_2 in a magmatic system is to measure the Fe^{3+}/Fe^{2+} ratio in minerals directly. For example, Luth and Canil (1993) proposed an oxybarometer based on Mössbauer spectroscopy analysis of Fe^{3+} and Fe^{2+} in Cpx of ultramafic rocks. Delaney et al. (1998) have shown that synchrotron micro-XANES probe can be used to measure Fe^{3+}/Fe^{2+} even in minerals like Pl that have only very small bulk iron contents. Thanks to this method, Tegner et al. (2003) constrained the fO_2 in the Skaergaard layered intrusion by measuring the Fe^{3+} contents in Pl. However, one problem in constraining the redox conditions of melt from Fe^{3+}/Fe^{2+} ratio in minerals is that the partition coefficient of Fe^{3+} and of Fe^{2+} between mineral and melt must be known (Tegner et al., 2003). For Pl, Sato (1989) and Phinney (1992) have proposed that the partition coefficient of FeO^{total} ($D^{Fe^{total}}_{Pl\text{-}melt}$) increases with the fO_2 due to substitution of Al_2O_3 in Pl by Fe_2O_3. Lundgaard and Tegner (2004), using the same thermodynamic model as Sugawara (2000, 2001), have shown that $D^{Fe3+}_{Pl\text{-}melt}$ is much larger than $D^{Fe2+}_{Pl\text{-}melt}$ (0.19–0.92 and 0.008–0.05, respectively), and that both depend on the melt composition. Consequently, Pl incorporates Fe^{3+} better than Fe^{2+}. These data also show that $D^{Fe2+}_{Pl\text{-}melt}$ and $D^{Fe3+}_{Pl\text{-}melt}$ do not depend on fO_2, while $D^{Fe\_total}_{Pl\text{-}melt}$ does consequently to the higher Fe^{3+} content of melt under oxidizing conditions. In Cpx, McCanta et al. (2004) give $F^{Fe3+}_{Cpx\text{-}melt}$ values ranging from 0 to 0.77. As Fe^{2+} in typical magmatic Cpx is a major element, it does not follow Henry's law, and partition coefficients should be used with caution. Nevertheless, for a precisely constrained compositional system, a rough estimate of an "apparent partition coefficient" (noted $D^{*Fe2+}_{Cpx\text{-}melt}$) can be made by the evaluation of available experimental data (see section "Controlling parameters").

Other methods are available to estimate the redox state of magmatic systems, such as measurements with the EELS technique (e.g., Van Aken et al., 1998; Van Aken and Liebscher, 2002). King et al. (2000) have shown that the partitioning of Fe^{3+}/Fe^{total} between amphibole and melt is close to unity and thus Fe^{3+} contents in amphibole reflect the redox state of the melt.

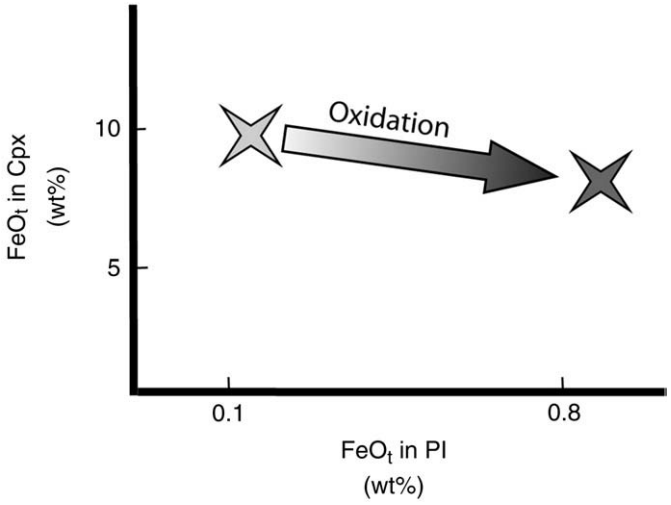

Fig. 1. Rationale for the proposed model. FeO^{total} decreases in Cpx and increases in Pl when the parental melt is oxidized.

Fialin et al. (2001, 2004) have shown that the Fe^{3+}/Fe^{total} of some minerals and glasses can be estimated with the electron microprobe using the self-absorption-induced shift of the Fe$L\alpha$ peak. Estimating the fO_2 from the partitioning of Eu between Pl and melt (Wilke and Behrens, 1999) or from the partitioning of V between olivine and melt (Canil, 1997) is also widely used.

A problem resulting from constraining the melt fO_2 from micro-XANES via synchrotron radiation, EELS, Mössbauer or trace element in plagioclase or olivine is that such facilities are not easily accessible to the whole community and cannot be used for routine analysis.

In the present paper we propose a new simple method to estimate the fO_2 of basalts based on microprobe analyses of two of the most common minerals of basaltic series (Pl and Cpx). This method does not include stoichiometric estimations based on formula calculations; it is restricted to basaltic systems under relatively oxidizing conditions ($\Delta FMQ > 0$). Hence, it is well-suited for an application to subduction zone-related basaltic series which are characterized by relatively oxidizing redox conditions (e.g., Johnson et al., 1994; Kelley and Cottrell, 2009). Moreover, since the presence of water has generally an oxidizing effect on the redox conditions (e.g., Botcharnikov et al., 2005), this method is also well-suited for an application to hydrous MORB-type systems, e.g., the melts produced at the gabbro/dike transition from fast-spreading mid-ocean ridges, where magmatic and hydrothermal reactions interfere (e.g., Nicolas et al., 2008; Koepke et al., 2008; France et al., 2009, 2010).

2. Model

The model presented here allows estimation of the redox conditions, expressed as the ΔFMQ at which a basaltic rock has crystallized, based on microprobe analyses of FeO_{total} in Cpx and Pl.

Our model is based on the different behaviour of the partitioning coefficients $K^{Cpx\text{-}melt}_{DFe_2O3/FeO}$ and $K^{Pl\text{-}melt}_{DFe_2O3/FeO}$. These K_Ds are equivalent to the ratio of the partition coefficient of Fe_2O_3 and FeO between Cpx and melt, and between Pl and melt, respectively: $K^{Cpx\text{-}melt}_{DFe_2O3/FeO} = D^{Fe3+}_{Cpx\text{-}melt}/D^{*Fe2+}_{Cpx\text{-}melt}$ and $K^{Pl\text{-}melt}_{DFe_2O3/FeO} = D^{Fe3+}_{Pl\text{-}melt}/D^{Fe2+}_{Pl\text{-}melt}$. In basaltic series the K_D are around 0.4 and 18 for Cpx and Pl, respectively (see the next section "Controlling parameters" for estimation of $D^{Fe3+}_{Cpx\text{-}melt}$, $D^{*Fe2+}_{Cpx\text{-}melt}$, $D^{Fe3+}_{Pl\text{-}melt}$ and $D^{Fe2+}_{Pl\text{-}melt}$). Thus, $D^{Fe3+}_{Cpx\text{-}melt}$ is lower than $D^{*Fe2+}_{Cpx\text{-}melt}$ and $D^{Fe3+}_{Pl\text{-}melt}$ is significantly higher than $D^{Fe2+}_{Pl\text{-}melt}$. Consequently, when a melt is oxidized (Fe^{2+} content decreases and Fe^{3+} content increases) FeO^{total} decreases in Cpx and increases in Pl (Fig. 1).

The ratio between the total iron contents in Cpx and Pl can be written as the ratio of the sums of ferric and ferrous iron in Cpx and Pl, respectively:

$$\frac{FeO^{total}_{Cpx}}{FeO^{total}_{Pl}} = \frac{Fe^{total}_{Cpx}}{Fe^{total}_{Pl}} = \frac{Fe^{3+}_{Cpx} + Fe^{2+}_{Cpx}}{Fe^{3+}_{Pl} + Fe^{2+}_{Pl}} \quad (1)$$

where FeO represents weight percents, and Fe moles. The partition coefficients ("*D*" for trace elements) and apparent partition coefficients ("*D**" for major element for a small range of melt composition) are defined by the relation: $D^{element}_{mineral\text{-}melt}=[conc.]_{mineral}/[conc.]_{melt}$.

Where "conc." is the concentration of the considered element (expressed either in moles or wt.%). By using partition coefficients, the ratio between the total iron contents in Cpx and Pl can be expressed from the composition of the melt:

$$\frac{FeO^{total}_{Cpx}}{FeO^{total}_{Pl}}=\frac{[(Fe^{3+}_{melt}\times D^{Fe3+}_{Cpx-melt})+(Fe^{2+}_{melt}\times D^{*Fe2+}_{Cpx-melt})]}{[(Fe^{3+}_{melt}\times D^{Fe3+}_{Pl-melt})+(Fe^{2+}_{melt}\times D^{Fe2+}_{Pl-melt})]}. \tag{2}$$

A factorisation of Eq. (2) leads to:

$$\frac{FeO^{total}_{Cpx}}{FeO^{total}_{Pl}}=\frac{\left[\left(D^{Fe3+}_{Cpx-melt}\times\frac{Fe^{3+}_{melt}}{Fe^{2+}_{melt}}\right)+D^{*Fe2+}_{Cpx-melt}\right]}{\left[\left(D^{Fe3+}_{Pl-melt}\times\frac{Fe^{3+}_{melt}}{Fe^{2+}_{melt}}\right)+D^{Fe2+}_{Pl-melt}\right]}. \tag{3}$$

A reorganization of Eq. (3) by using the relation (4) (where M_{FeO} and M_{Fe2O3} are the molar masses of the oxides: 71.85 and 159.69 g/mol, respectively) leads to Eq. (5):

$$\frac{Fe^{3+}_{melt}}{Fe^{2+}_{melt}}=\left(\frac{Fe_2O_3}{FeO}\right)_{melt}\times\frac{M_{FeO}\times 2}{M_{Fe_2O_3}} \tag{4}$$

$$\left(\frac{Fe_2O_3}{FeO}\right)_{melt}=\frac{D^{*2+}_{Cpx-melt}-\left(\frac{FeO^{total}_{Cpx}}{FeO^{total}_{Pl}}\times D^{2+}_{Pl-melt}\right)}{-D^{3+}_{Cpx\_melt}+\left(\frac{FeO^{total}_{Cpx}}{FeO^{total}_{Pl}}\times D^{3+}_{Pl-melt}\right)}\times\frac{M_{Fe2O3}}{M_{FeO}\times 2}. \tag{5}$$

Eq. (5) links the Fe_2O_3/FeO ratio of the melt to the total iron contents of the Cpx and Pl for a set of parameters (partitions coefficients and molar masses). The Fe_2O_3/FeO ratio is directly linked to the oxidation state of the melt. According to Kress and Carmichael (1991) the Fe_2O_3/FeO ratio of the melt is linked to its fO_2 and can be estimated by the empirical relation:

$$\log(fO_2)=\log\left\{\exp\left(\frac{\ln\left(\frac{Fe_2O_3}{FeO}\right)_{melt}-\frac{b}{T}-c-\sum_i diXi}{a}\right)\right\} \tag{6}$$

with $a=0.207$; $b=12\,980$; $c=-6.115$; $d_{SiO2}=-2.368$; $d_{Al2O3}=-1.622$ and $d_{CaO}=2.073$. With T the temperature in K and Xi between 0 and 1 calculated from oxides (in wt.%). The Eq. (7) from Kress and Carmichael (1991) should be used if high pressure and high temperature (>1630°) are considered:

$$\log(fO_2)=\log\left\{\exp\left(\frac{\ln\left(\frac{Fe_2O_3}{FeO}\right)_{melt}-\frac{b}{T}-c-\sum_i diXi-e\left[1-\frac{T_0}{T}-\ln\left(\frac{T}{T_0}\right)\right]-f\frac{P\times 10^9}{T}-g\frac{(T-T_0)P\times 10^9}{T}-h\frac{(P\times 10^9)^2}{T}}{a}\right)\right\} \tag{7}$$

with $a=0.196$; $b=11\ 492$; $c=-6.675$; $e=-3.36$; $f=-7.01$ 10–7; $g=-1.54$ 10–10; $h=3.85$ 10–17; $d_{Al2O3}=-2.243$; $d_{FeO*}=-1.828$; $d_{CaO}=3.201$; $d_{Na2O}=5.854$; $d_{K2O}=6.215$ and $T_0=1673$. With P the pressure in GPa and T in K and Xi between 0 and 1.

Ottonello et al. (2001) proposed a new thermodynamic model for calculating the oxidation state of Fe in dry silicate melts and glasses at atmospheric pressure. Moretti (2005) extended this model considering the effect of pressure and water content. In Figure 12 shot, Botcharnikov et al. (2005) showed that the differences between these different models are small. The use of the model proposed by Moretti (2005) is restricted to melt of known water content. However, since the water content of those natural melts crystallizing plagioclase and pyroxene is generally unknown, the general application of the model of Moretti (2005) is hampered. Therefore, we use the model of Kress and Carmichael (1991).

The redox state of a melt can be better understood by comparing the fO_2 to oxygen buffers. We recall here the relations corresponding to the FMQ (Eq. (8)) and to the NNO oxygen buffers (where NNO is the Ni–NiO solid oxygen buffer equilibrium; Eq. (9)) from Ballhaus et al. (1991):

$$\Delta FMQ=\log fO_2-(82.75+0.00484T-30681/T-24.45\log T+940P/T-0.02P) \tag{8}$$

$$\Delta NNO=\log fO_2-(12.78-25073/T-1.1\log T+450P/T+0.025P) \tag{9}$$

From Eqs. (8) and (9) the redox state of a melt can be obtained by knowing P, T, the composition of the melt, and the composition in total iron of Cpx and Pl (FeO^{total}_{Cpx} and FeO^{total}_{Pl}). We provide an EXCEL spreadsheet (Supplementary material) in order to facilitate the use of Eqs. (5), (6) and (8). The estimation of partition coefficients $D^{Fe3+}_{Cpx-melt}$, $D^{Fe3+}_{Pl-melt}$, $D^{Fe2+}_{Pl-melt}$ and apparent partition coefficient $D^{*Fe2+}_{Cpx-melt}$ is discussed in the following.

2.1. Controlling parameters

To estimate the redox state of a melt with the model presented here, it is necessary to know the partition coefficients $D^{Fe3+}_{Pl-melt}$, $D^{Fe2+}_{Pl-melt}$, $D^{Fe3+}_{Cpx-melt}$ and apparent partition coefficient $D^{*\ Fe2+}_{Cpx-melt}$ (Eq. (5)).

We estimate these parameters by evaluating the existing literature data. It should be noted that the accuracy of our model can be improved in the future, with new data on partition coefficients.

$D^{Fe3+}_{Pl-melt}$ and $D^{Fe2+}_{Pl-melt}$ can be calculated from the melt composition by using Eq. (10) determined by Lundgaard and Tegner (2004):

$$\ln(D) = a + \sum_i biXi. \quad (10)$$

Parameters determined by Lundgaard and Tegner (2004) for Eq. (10) are summarized in Table 1 (with *Xi* in wt.%).

$D^{*Fe2+}_{Cpx-melt}$ and $D^{Fe3+}_{Cpx-melt}$ remain poorly constrained in literature. As recalled in the introduction, a prerequisite for the estimation of $D^{*Fe2+}_{Cpx-melt}$ is to identify the compositional field of interest, since $D^{*Fe2+}_{Cpx-melt}$ is strongly dependent on the composition of the system. Because our study focuses on basaltic systems, we derive $D^{*Fe2+}_{Cpx-melt}$ empirically by evaluating experimental data in basaltic and andesitic systems with SiO_2<60 wt.%. For this, we use the studies of Snyder et al. (1993), Toplis et al. (1994), Toplis and Carroll (1995), Berndt et al. (2005), Freise et al. (2009), Botcharnikov et al. (2008), and unpublished data from S. Feig. Based on more than 100 experiments, $D^{*Fe2+}_{Cpx-melt}$ has been regressed against the melt composition, temperature, and pressure (R^2 = 0.81; Fig. 2) according to:

$$D^{*Fe2+}_{Cpx-melt} = a + \sum_i biXi. \quad (11)$$

Parameters determined for Eq. (11) are summarized in Table 1 (with *Xi* in wt.%). Because we use only experimental data from reducing experiments (ΔFMQ<0), we assume that Fe^{3+} has a negligible influence on Fe^{total} in melt and Cpx, and the estimated apparent partition coefficient is therefore a good approximation for the case of ferrous iron. Several studies on basaltic series (e.g., Dale and Henderson, 1972; Bougault and Hekinian, 1974; Jones and Layne, 1997) have bracketed $D^{*Fe2+}_{Cpx-melt}$ between 0.714 and 1, which is in agreement with Fig. 2.

To estimate $D^{Fe3+}_{Cpx-melt}$, we use the work of McCanta et al. (2004), who performed experiments at reducing conditions (ΔFMQ varies between −5.0 and 0.5), and measured the Fe^{3+} content of melt and Cpx with XANES technique, and calculated the associated $D^{Fe3+}_{Cpx-melt}$. To date, no other data on $D^{Fe3+}_{Cpx-melt}$ is available. $D^{Fe3+}_{Cpx-melt}$ varies from 0 to 0.77 (5 measurements) with standard deviations up to 0.7 (McCanta et al., 2004). Despite $D^{Fe3+}_{Cpx-melt}$ seems to increase with more oxidizing conditions (McCanta et al., 2004), and because of the very large standard deviations in these results, we propose to use here the average value (0.27) of McCanta et al. (2004) data with a large associated error (±0.27).

2.2. Limitations

The model is valid for Cpx–Pl pairs crystallized under equilibrium conditions; the use of skeletal or dendritic crystals is therefore not recommended. As iron is a trace to minor element in Pl, long counting times should be used with the electron microprobe. Lundgaard and Tegner (2004) shown that analyses of small Pl grains (<5 μm) in experimental charges are poorly relevant because of a secondary fluorescence from iron in the host glass that increase the FeO_t in Pl, larger grains should therefore be used. As the partition coefficients are derived from basaltic series with SiO_2<60%, the model should be restricted to such compositions. Moreover, it has been developed for lavas, and since the partition coefficients have been derived from experiments performed under shallow pressures ranging between 10^{-4} GPa (1 atm) and 0.5 GPa, we recommend using the model within this pressure interval. To apply this model to other systems or pressures, a re-evaluation of the corresponding partition coefficients is necessary.

Another important limitation comes from the concept of the model itself. Discriminating between reducing and oxidizing conditions is possible because of the different partitioning behaviour of Fe^{3+} with respect to Pl/melt and Cpx/melt. Since under reducing conditions, the Fe^{3+} content of the melt is very small, the error in the estimation increases drastically. Therefore, we recommend application of the model only to relatively oxidizing conditions with an oxygen fugacity equal to, or higher than, the FMQ oxygen buffer.

2.3. Error propagation analysis

For $D^{Fe3+}_{Cpx-melt}$ the used associated errors is large (±0.27) to account for the poor constrains on this parameters. Errors on FeO^{total}_{Cpx}, FeO^{total}_{Pl}, melt composition, *T* and *P* are also considered in the error propagation analysis. The error propagation analysis has been performed following Ku (1966) by considering all variables as independent (independent measurements). Details of the calculation are summarized in the Appendix A. The error propagation analysis is also included in the spreadsheet provided as supplementary material. The error propagation analysis results highlight that the error on melt composition, *T* and *P* have a small influence on the whole calculated error; rough estimation of these parameters can therefore be used.

Table 1
Parameters determined by Lundgaard and Tegner (2004) to use in Eq. (10), and determined in this study to use in Eq. (11).

	Eq. (10)				Eq. (11)
	Sub-alkaline		Alkaline		
	$\ln(D^{Fe_2O_3}_{Pl-melt})$	$\ln(D^{FeO}_{Pl-melt})$	$\ln(D^{Fe_2O_3}_{Pl-melt})$	$\ln(D^{FeO}_{Pl-melt})$	$D^{*Fe2+}_{Cpx-melt}$
Regression coefficients b_i					
SiO_2	0.0167	0.00298	0.0176	0.0655	0.01286
TiO_2	−0.0578	−0.0201	−0.0509	0.0205	−0.05039
Al_2O_3	−0.0394	−0.0589	−0.0395	−0.0155	−0.08028
FeO^{total}	−0.0779	−0.0559	−0.107	0.0115	−0.05332
MgO	−0.0295	−0.107	−0.0872	−0.0363	−0.01634
CaO	−0.000558	−0.00484	−0.0252	0.100	−0.02799
Na_2O	−0.0292	−0.140	−0.114	0.0122	−0.03103
K_2O	0.130	−0.0430	0.0530	0.0642	0.05440
–	–	–	–	–	–
T	0	0	0	0	−0.00113
P	0	0	0	0	0.54644
–	–	–	–	–	–
a	−0.211	−1.555	0.980	−8.263	4.04688

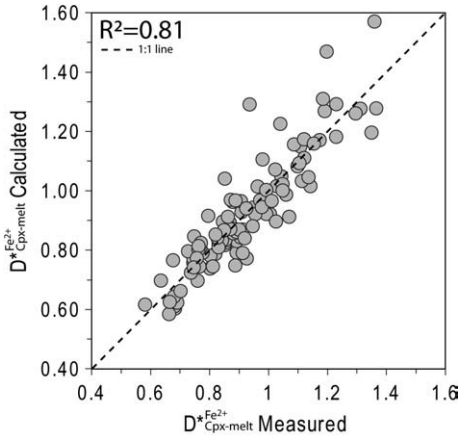

Fig. 2. $D^{*Fe2+}_{Cpx-melt}$ calculated with Eq. (11) vs. $D^{*Fe2+}_{Cpx-melt}$ measured in experiments used for the regression of Eq. (11). Selected experiments are performed under reducing conditions. Data are from Snyder et al. (1993), Toplis et al. (1994), Toplis and Carroll (1995), Berndt et al. (2005), Freise et al. (2009), Botcharnikov et al. (2008), and Feig (personal communication). The dashed line is the 1:1 line. The accuracy of the parameterization is attested by the $R^2 = 0.81$.

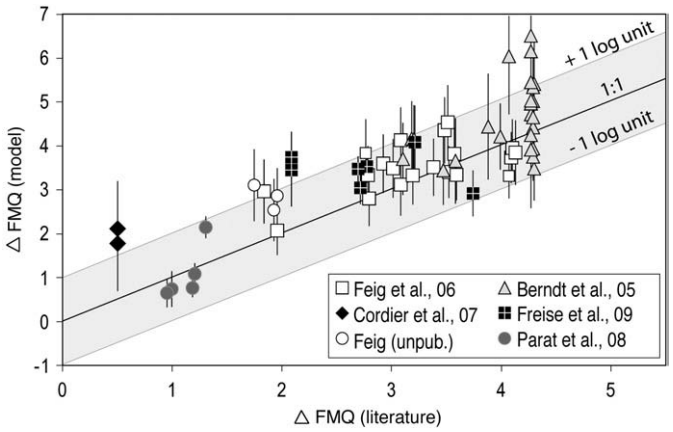

Fig. 3. Comparison of oxygen fugacity expressed in log units relative to the FMQ oxygen buffer calculated with our model and given in literature for the same data. Data are from Berndt et al. (2005), Feig et al. (2006), Cordier et al. (2007), Parat et al. (2008), Freise et al. (2009), and Feig et al. (personal communication). Error bars are those for values calculated with the error propagation analysis of our model (2σ). Most of the calculated values are consistent with literature in the range of ±1 log unit (shaded area), which corresponds to the average standard deviation calculated with the model.

3. Model testing

In order to test our model, we have selected a set of natural and experimental data (Fig. 3), where Cpx, Pl and melt compositions are given together with an estimate of the redox state for basaltic compositions with SiO_2 contents below 60 wt.%. For natural data, we use the study of Cordier et al. (2007) on samples from the Blanco Deep on the East Pacific Rise. Experimental data are taken from Berndt et al. (2005), Feig et al. (2006), Freise et al. (2009), Parat et al. (2008), and Feig (personal communication). It should be noted that the experimental data from Berndt et al. (2005), Freise et al. (2009), and Feig (personal communication) used in Fig. 2 for calibration under reducing condition are not the same as those under oxidizing conditions used here to test the model.

Taking into account the errors calculated with our model (2σ), most of the calculated oxygen fugacity expressed in log units relative to the FMQ oxygen buffer are in good agreement with the published ones (Fig. 3).

4. Conclusion

The model presented here allows us to estimate the redox state in basaltic rocks that contain plagioclase and clinopyroxene. It is based on the different partitioning behaviour of ferric and ferrous iron between clinopyroxene and melt and plagioclase and melt. Input data are FeO_{total} contents of these minerals which can be easily measured using an electron microprobe, an estimate of melt composition, and approximate equilibrium temperature. The application of our model is restricted to basaltic series containing less than 60% of SiO_2 equilibrated under shallow pressures and under oxidizing conditions (ΔFMQ>0). The accuracy of this method is about ±1 log unit, and the exact associated error can easily be calculated along with the ΔFMQ using a spreadsheet provided within the supplementary material.

Acknowledgments

Ariel Provost (LMV, Clermont-Ferrand, France) is thanked for checking the error propagation analysis. Carole Cordier (MNA, Siena, Italy) is thanked for providing unpublished data and for discussions. Roberto Moretti (INVG, Naples, Italy) is thanked for providing the software associated with his redox determination model that has been used in the first steps of elaboration of our model. Constructive reviews by Bernard W. Evans, Robert W. Luth, and an anonymous reviewer are gratefully acknowledged. Editorial advice from Malcolm J. Rutherford is acknowledged.

Appendix A. Error propagation analysis

Error associated to the ΔFMQ value obtained with Eqs. ((8), (6), (5)) can be calculated using the equation:

$$\sigma^2_{\Delta FMQ} = \left[\frac{\partial \Delta_{FMQ}}{\partial Sc}\times\sigma_{Sc}\right]^2 + \left[\frac{\partial \Delta_{FMQ}}{\partial Sp}\times\sigma_{Sp}\right]^2 + \left[\frac{\partial \Delta_{FMQ}}{\partial D^{+++}_{Cpx-melt}}\times\sigma_{D^{+++}_{Cpx-melt}}\right]^2 + \left[\frac{\partial \Delta_{FMQ}}{\partial P}\times\sigma_{P}\right]^2 + \left[\frac{\partial \Delta_{FMQ}}{\partial T}\times\sigma_{T}\right]^2 + \left[\frac{\partial \Delta_{FMQ}}{\partial Xi}\times\sigma_{Xi}\right]^2$$

where *Sc* and *Sp* represent the FeO^{total} content of clinopyroxene and plagioclase, respectively.

With:

$$\frac{\partial \Delta_{FMQ}}{\partial Sc} = \frac{1}{a\ln 10}\left\{\frac{\left(1/Sp\right)\left(D^{+++}_{Cpx-melt}D^{++}_{Pl-melt} - D^{+++}_{Pl-melt}D^{++}_{Cpx-melt}\right)}{\left[-D^{+++}_{Cpx-melt} + \left(\frac{Sc}{Sp}\times D^{+++}_{Pl-melt}\right)\right]\left[D^{++}_{Cpx-melt} - \left(\frac{Sc}{Sp}\times D^{++}_{Pl-melt}\right)\right]}\right\}$$

$$\frac{\partial \Delta_{FMQ}}{\partial Sp} = \frac{1}{a\ln 10}\left\{\frac{\left(Sc/Sp^2\right)\left(D^{+++}_{Pl-melt}D^{++}_{Cpx-melt} - D^{+++}_{Cpx-melt}D^{++}_{Pl-melt}\right)}{\left[-D^{+++}_{Cpx-melt} + \left(\frac{Sc}{Sp}\times D^{+++}_{Pl-melt}\right)\right]\left[D^{++}_{Cpx-melt} - \left(\frac{Sc}{Sp}\times D^{++}_{Pl-melt}\right)\right]}\right\}$$

$$\frac{\partial \Delta_{FMQ}}{\partial D^{+++}_{Cpx-melt}} = \frac{1}{a\ln 10} \times \frac{1}{\left[-D^{+++}_{Cpx-melt} + \left(Sc/_{Sp} \times D^{+++}_{Pl-melt}\right)\right]}$$

$$\frac{\partial \Delta_{FMQ}}{\partial P} = \left[\frac{1}{a\ln 10} \times \left(\frac{b_P}{\left[D^{++}_{Cpx-melt} - \left(Sc/_{Sp} \times D^{++}_{Pl-melt}\right)\right]} + \frac{b}{T^2}\right)\right] - \frac{940}{T} + 0.02$$

Where $b_P = bi$ for pressure in Eq. (11);

$$\frac{\partial \Delta_{FMQ}}{\partial T} = \left[\frac{1}{a\ln 10} \times \left(\frac{b_T}{\left[D^{++}_{Cpx-melt} - \left(Sc/_{Sp} \times D^{++}_{Pl-melt}\right)\right]} + \frac{b}{T^2}\right)\right] - 0.00484 + \frac{30681}{T^2} + \frac{24.45}{T\ln 10} + \frac{940P}{T^2}$$

where $b_T = bi$ for temperature in Eq. (11);

$$\frac{\partial \Delta_{FMQ}}{\partial Xi} = \frac{1}{a\ln 10} \times \left\{\left[\frac{\left\{\left[gi - \left(ki \times Sc/_{Sp} \times D^{++}_{Pl-melt}\right)\right] \times \left[-D^{+++}_{Cpx-melt} + \left(Sc/_{Sp} \times D^{+++}_{Pl-melt}\right)\right]\right\} - \left\{\left[D^{++}_{Cpx-melt} - \left(Sc/_{Sp} \times D^{++}_{Pl-melt}\right)\right] \times \left[mi \times \left(Sc/_{Sp} \times D^{+++}_{Pl-melt}\right)\right]\right\}}{\left[D^{++}_{Cpx-melt} - \left(Sc/_{Sp} \times D^{++}_{Pl-melt}\right)\right] \times \left[-D^{+++}_{Cpx-melt} + \left(Sc/_{Sp} \times D^{+++}_{Pl-melt}\right)\right]}\right] + di/_{100}\right\}$$

where $g_i = b_i$ in Eq. (11) for $D^{*Fe2+}_{Cpx-melt}$; $k_i = b_i$ in Eq. (10) for $D^{Fe2+}_{Pl-melt}$; $m_i = b_i$ in Eq. (10) for $D^{Fe3+}_{Pl-melt}$.

Appendix B. Supplementary data

Supplementary data associated with this article can be found, in the online version, at doi:10.1016/j.jvolgeores.2009.11.023.

References

Andersen, D.J., Lindsley, D.H., 1985. New (and final!) models for the Ti-magnetite/ilmenite geothermometer and oxygen barometer. Abstract AGU 1985 Spring Meeting Eos Transactions. American Geophysical Union, pp. 66–416.

Bacon, C.R., Hirschmann, M.M., 1988. Mg/Mn partitioning as a test for equilibrium between coexisting Fe–Ti oxides. Am. Mineral. 73, 57–61.

Ballhaus, C., 1993. Redox states of lithospheric and asthenospheric upper mantle. Contrib. Mineral. Petrol. 114, 331–348.

Ballhaus, C., Frost, B.R., 1994. The generation of oxidized CO_2-bearing basaltic melts from reduced CH_4-bearing upper mantle sources. Geochim. Cosmochim. Acta 58, 4931–4940.

Ballhaus, C., Berry, R.F., Green, D.H., 1991. High pressure experimental calibration of the olivine–orthopyroxene–spinel oxygen geobarometer: implications for the oxidation state of the upper mantle. Contrib. Mineral. Petrol. 107, 27–40.

Basaltic Volcanism Study Project, 1981. Temperature and Gas Fugacities of Planetary Basalts. Pergamon Press Inc., New York, pp. 371–384.

Berndt, J., Koepke, J., Holtz, F., 2005. An experimental investigation of the influence of water and oxygen fugacity on differentiation of MORB at 200 MPa. J. Petrol. 46, 135–167.

Botcharnikov, R.E., Koepke, J., Holtz, F., McCammon, C., Wilke, M., 2005. The effect of water activity on the oxidation and structural state of Fe in a ferro-basaltic melt. Geochim. Cosmochim. Acta 69, 5071–5085.

Botcharnikov, R.E., Almeev, R.R., Koepke, J., Holtz, F., 2008. Phase relations and liquid lines of descent in hydrous ferrobasalt—implications for the Skaergaard intrusion and Columbia River flood basalts. J. Petrol. 49–9, 1687–1727.

Bougault, H., Hekinian, R., 1974. Rift valley in the Atlantic Ocean near 36 degrees 50′N; petrology and geochemistry of basalt rocks. Earth Planet. Sci. Lett. 24, 249–261.

Brett, R., Sato, M., 1984. Intrinsic oxygen fugacity measurements on seven chondrites, a pallasite, and a tektite and the redox state of meteorite parent bodies. Geochim. Cosmochim. Acta 48, 111–120.

Buddington, A.F., Lindsley, D.H., 1964. Iron–titanium oxide minerals and synthetic equivalents. J. Petrol. 5, 310–357.

Canil, D., 1997. Vanadium partitioning and the oxidation state of Archaean komatiite magmas. Nature 389, 842–845.

Canil, D., O'Neill, H.St.C., 1996. Distribution of ferric iron in some upper-mantle assemblages. J. Petrol. 37, 609–635.

Carmichael, I.S.E., 1991. The redox state of basic and silicic magmas: a reflection of their source regions? Contrib. Mineral. Petrol. 106, 129–141.

Carmichael, I.S.E., Ghiorso, M.S., 1986. Oxidation-reduction in basic magmas: a case for homogeneous equilibria. Earth Planet. Sci. Lett. 78, 200–210.

Cordier, C., Caroff, M., Juteau, T., Fleutelot, C., Hémond, C., Drouin, M., Cotton, J., Bollinger, C., 2007. Bulk-rock geochemistry and plagioclase zoning in lavas exposed along the northern flank of the Western Blanco Depression (Northeast Pacific): insight into open-system magma chamber processes. Lithos 99, 289–311.

Dale, I.M., Henderson, P., 1972. The partition of transition elements in phenocryst-bearing basalts and the implications about melt structure. 24th Int Geol Congr Sect, vol. 10, pp. 105–111.

Delaney, J.S., Dyar, M.D., Sutton, S.R., Bajt, S., 1998. Redox ratio with relevant resolution; solving an old problem by using the synchrotron micro-XANES probe. Geology 26, 139–142.

Feig, S.T., Koepke, J., Snow, J.E., 2006. Effect of water on tholeiitic basalt phase equilibria: an experimental study under oxidizing conditions. Contrib. Mineral. Petrol. 152, 611–638.

Fialin, M., Wagner, C., Métrich, N., Humler, E., Galoisy, L., Bézos, A., 2001. Fe^{3+}-ΣFe vs. Fe Lα peak energy for minerals and glasses: recent advances with electron microprobe. Am. Mineral. 86, 456–465.

Fialin, M., Bézos, A., Wagner, C., Magnien, V., Humler, E., 2004. Quantitative electron microprobe analysis of Fe^{3+}-ΣFe: basic concepts and experimental protocol for glasses. Am. Mineral. 89, 654–662.

France, L., Ildefonse, B., Koepke, J., 2009. Interactions between magma and hydrothermal system in Oman ophiolite and in IODP Hole 1256D: fossilization of a dynamic melt lens at fast spreading ridges. Geochem. Geophys. Geosyst. 10–10, Q10O19. doi:10.1029/2009GC002652.

France, L., Koepke, J., Ildefonse, B., Cichy, S.B., Deschamps, F., 2010. Hydrous partial melting in the sheeted dike complex at fast spreading ridges: experimental and natural observations. Accepted to Contrib. Mineral. Petrol.

Freise, M., Holtz, F., Nowak, M., Scoates, J.S., Strauss, H., 2009. Differentiation and crystallization conditions of basalts from the Kerguelen large igneous province: an experimental study. Contrib. Mineral. Petrol. on line first doi:10.1007/s00410-009-0394-5.

Ghiorso, M.S., Evans, B.W., 2008. Thermodynamics of rhombohedral oxide solid solutions and a revision of the Fe–Ti two-oxide geothermometer and oxygen-barometer. Am. J. Sci. 308–9, 957–1039.

Ghiorso, M.S., Sack, R.O., 1991. Fe–Ti oxide geothermometry: thermodynamic formulation and the estimation of intensive variables in silicic magmas. Contrib. Mineral. Petrol. 108, 485–510.

Ginibre, C., Wörner, G., Kronz, A., 2002. Minor- and trace-element zoning in plagioclase: implications for magma chamber processes at Parinacota volcano, northern Chile. Contrib. Mineral. Petrol. 143, 300–315.

Grove, T.L., Baker, M.B., 1984. Phase equilibrium controls on the tholeiitic versus calc-alkaline differentiation trends. J. Geophys. Res. 85, 3253–3274.

Herd, C.D.K., 2008. Basalts as probes of planetary interior redox state. Rev. Mineral. Geochem. 68, 527–553. doi:10.2138/rmg.2008.68.19.

Johnson, M.C., Anderson, A.T., Rutherford, M.J., 1994. Pre-eruptive volatile contents of magmas. In: Carroll, M.R., Holloway, J.R. (Eds.), Volatiles in magmas. Rev. Mineral., vol. 30. Mineralogical Society of America, Washington, DC, United States, pp. 281–330.

Jones, R.H., Layne, G.D., 1997. Minor and trace element partitioning between pyroxene and melt in rapidly cooled chondrules. Am. Mineral. 82, 534–545.

Kelley, K.A., Cottrell, E., 2009. Water and the oxidation state of subduction zone magmas. Science 325, 605–607. doi:10.1126/science.1174156.

Kilinc, A., Carmichael, I.S.E., Rivers, M.L., Sack, R.O., 1983. The ferric-ferrous ratio of natural silicate liquids equilibrated in air. Contrib. Mineral. Petrol. 83, 136–140.

King, P.L., Hervig, R.L., Holloway, J.R., Delaney, J.S., Dyar, M.D., 2000. Partitioning of Fe^{3+}–Fe_{total} between amphibole and basanitic melt as a function of oxygen fugacity. Earth Planet. Sci. Lett. 178, 97–112.

Koepke, J., Christie, D.M., Dziony, W., Holtz, F., Lattard, D., Maclennan, J., Park, S., Scheibner, B., Yamasaki, T., Yamazaki, S., 2008. Petrography of the dike/gabbro transition at IODP site 1256 (Equatorial Pacific): the evolution of the granoblastic dikes. Geochem. Geophys. Geosyst., 9–7, p. Q07O09. doi:10.1029/2008GC001939.

Kress, V.C., Carmichael, I.S.E., 1991. The compressibility of silicate liquids containing Fe_2O_3 and the effect of composition, temperature, oxygen fugacity and pressure on their redox states. Contrib. Mineral. Petrol. 108, 82–92.

Ku, H., 1966. Notes on the use of propagation of error formulas. J. Res. Natl. Bur. Stand., C Eng. Instrum. 70C (4), 263–273.
Kuritani, T., 1998. Boundary layer crystallisation in a basaltic magma chamber: evidence from Rishiri volcano, Northern Japan. J. Petrol. 39, 1619–1640.
Lundgaard, K.L., Tegner, C., 2004. Partitioning of ferric and ferrous iron between plagioclase and silicate melt. Contrib. Mineral. Petrol. 147, 470–483.
Luth, R.W., Canil, D., 1993. Ferric iron in mantle-derived pyroxenes and a new oxybarometer for the mantle. Contrib. Mineral. Petrol. 113, 236–248.
McCanta, M.C., Dyar, M.D., Rutherford, M.J., Delaney, J.S., 2004. Iron partitioning between basaltic melts and clinopyroxene as a function of oxygen fugacity. Am. Mineral. 89, 1685–1693.
Moretti, R., 2005. Polymerization, basicity, oxidation state and their role in ionic modelling of silicate melts. Ann. Geophys. 48, 583–608.
Nicolas, A., Boudier, F., Koepke, J., France, L., Ildefonse, B., Mevel, C., 2008. Root zone of the sheeted dike complex in the Oman ophiolite. Geochem. Geophys. Geosyst. 9, Q05001. doi:10.1029/2007GC001918.
Ottonello, G., Moretti, R., Marini, L., Zuccolini, M.V., 2001. Oxidation state of iron in silicate glasses and melts: a thermochemical model. Chem. Geol. 174, 157–179.
Parat, F., Holtz, F., Feig, S., 2008. Pre-eruptive conditions of the Huerto andesite (Fish canyon system, San Juan volcanic field, Colorado): influence of volatiles (C–O–H–S) on phase equilibria and mineral composition. J. Petrol. 49–5, 911–935.
Phinney, W.C., 1992. Partition coefficients for iron between plagioclase and basalts as a function of oxygen fugacity: implications for Archean and lunar anorthosites. Geochim. Cosmochim. Acta 56, 1885–1895.
Rhodes, J.M., Vollinger, M.J., 2005. Ferric/Ferrous ratio in 1984 Mauna Loa lavas: a contribution to understanding the oxidation state of Hawaiian magmas. Contrib. Mineral. Petrol. 149, 666–674.
Sato, H., 1989. Mg–Fe partitioning between plagioclase and liquid in basalts of Hole 504B, ODP Leg 111: a study of melting at 1 atm. Proc. Ocean Drill. Program Sci. Results 111, 17–26.
Sauerzapf, U., Lattard, D., Burchard, M., Engelmann, R., 2008. The titanomagnetite–ilmenite equilibrium: new experimental data and thermo-oxybarometric application to the crystallisation of basic to intermediate rocks. J. Petrol. 49–6, 1161–1185.
Snyder, D., Carmichael, I.S.E., Wiebe, R.A., 1993. Experimental study of liquid evolution in an Fe-rich, layered mafic intrusion: constraints of Fe–Ti oxide precipitation on the T-f_{O2} and T-ρ paths of tholeiitic magmas. Contrib. Mineral. Petrol. 113, 73–86.
Sobolev, V.N., McCammon, C.A., Taylor, L.A., Snyder, G.A., Sobolev, N.V., 1999. Precise Moessbauer milliprobe determination of ferric iron in rock-forming minerals and limitations of electron microprobe analysis. Am. Mineral. 88, 1145–1152.
Sugawara, T., 2000. Thermodynamic analysis of Fe and Mg partitioning between plagioclase and silicate liquid. Contrib. Mineral. Petrol. 138, 101–113.
Sugawara, T., 2001. Ferric iron partitioning between plagioclase and silicate liquid: thermodynamics and petrologicaly applications. Contrib. Mineral. Petrol. 141, 659–686.
Tegner, C., Delaney, J.S., Dyar, M.D., Lundgaard, K.L., 2003. Iron in Plagioclase as a monitor of oxygen fugacity in Skaergaard, Bushveld and Bjerkreim–Sokndal layered intrusions, and anorthosite of the Rogaland igneous province. Geophys. Res. Abstr. 5, 08789.
Toplis, M.J., Carroll, M.R., 1995. An experimental study of the influence of oxygen fugacity on Fe–Ti oxide stability, phase relations, and mineral-melt equilibria in ferro-basaltic systems. J. Petrol. 36–5, 1137–1170.
Toplis, M.J., Libourel, G., Carroll, M.R., 1994. The role of phosphorus in crystallisation processes of basalt: an experimental study. Geochim. Cosmochim. Acta 58–2, 797–810.
Van Aken, P.A., Liebscher, B., 2002. Quantification of ferrous/ferric ratio in minerals: new evaluation schemes of Fe L_{23} electron energy-loss near-edge spectra. Phys. Chem. Miner. 29, 188–200.
Van Aken, P.A., Liebscher, B., Styrsa, V.J., 1998. Quantitative determination of iron oxidation states in minerals using Fe L2, 3-edge electron energy-loss near-edge structure spectroscopy. Phys. Chem. Miner. 25, 323–327.
Venezky, D.Y., Rutherford, M.J., 1999. Petrology and Fe–Ti oxide reequilibration of the 1991 Mount Unzen mixed magma. J. Volcanol. Geotherm. Res. 89, 213–230.
Wilke, M., Behrens, H., 1999. The dependence of the partitioning of iron and europium between plagioclase and hydrous tonalitic melt on oxygen fugacity. Contrib. Mineral. Petrol. 137, 102–114.
Wood, B.J., Bryndzia, L.T., Johnson, K.E., 1990. Mantle oxidation state and its relationship to tectonic environment and fluid speciation. Science 248, 337–345.